Chemoproteomics-Enabled De Novo Discovery of Metallothionein Degraders Facilitates Probing Its Role in Cancer

Brittney Racioppo[†#], Dany Pechalrieu[†], Daniel Abegg[†], Brendan Dwyer[#], Neal Ramseier[†], Ying Hu[†], and Alexander Adibekian[†‡▽§$]

[†] Department of Chemistry, University of Illinois Chicago, 845 W Taylor Street, Chicago, IL 60607, USA
[‡]University of Illinois Cancer Center, 818 South Wolcott Avenue, Chicago, IL 60612, USA
[▽]UICentre, University of Illinois Chicago, 833 S. Wood Street, Chicago, IL 60612, USA
[§] Department of Pharmaceutical Sciences, University of Illinois Chicago, 833 S Wood Street, Chicago, IL 60607, USA
[$]Department of Biochemistry and Molecular Genetics, University of Illinois, 900 S Ashland Ave, Chicago, IL 60607, USA
[#]Skaggs Doctoral Program in the Chemical and Biological Sciences, Scripps Research, 10550 N Torrey Pines Road, La Jolla, CA 92037, USA

Abstract: Proteolysis targeting chimeras (PROTACs) represent powerful tools to modulate the activity of classically "undruggable" proteins, but their application has been limited to known ligands and a few select protein classes. Herein, we present our chemoproteomic strategy for *de novo* discovery of PROTAC degraders. Using comparative PROTAC versus ligand global proteomics analyses, we rapidly identify proteins selectively downregulated by "untargeted" PROTAC probes containing an E3 ligase recruiter and various cysteine-reactive protein-of-interest (POI) ligands. In this manuscript, we showcase our approach by identifying a first-in-class acrylamide- and VHL-based PROTAC for metallothionein 2A (MT2A) – a small, cysteine-rich, metal-binding protein implicated in heavy metal detoxification, zinc homeostasis, and cellular metastasis. Notably, isoform-specific MT overexpression has been shown to augment cellular migration and invasion across several cancer cell lines, though precise mechanisms are unknown due to insufficient tools to study MTs. We show that optimized PROTAC AA-BR-157 covalently binds conserved C44, degrades overexpressed MT2A with nanomolar potency, and reduces migration and invasion of triple negative breast cancer MDA-MB-231 cells. We further demonstrate a time-dependent increase in intracellular zinc levels following MT2A degradation as well as downregulation of protein diaphanous homolog 3 (DIAPH3), a positive regulator of actin and cell motility. Super-resolution imaging of MDA-MB-231 cells shows that downregulation of MT2A and DIAPH3 inhibits cell polarization and thereby migration, suggesting that MT2A regulates motility via DIAPH3-dependent cytoskeletal remodeling. In summary, our strategy enables the discovery of PROTACs for novel disease-related targets and lays the groundwork for expansion of the druggable proteome.

Introduction

Targeted protein degradation (TPD) has emerged as a formidable approach to modulate the function of classically "undruggable" proteins, such as intrinsically disordered proteins.[1-3] This method leverages event-driven pharmacology to achieve protein degradation and complete abolishment of protein activity. TPD offers significant advantages over direct inhibition, including a broader target range and prolonged duration of action.[3-6] A key strategy in TPD utilizes heterobifunctional proteolysis-targeting chimeras (PROTACs) to recruit E3 ubiquitin ligases to proteins-of-interest (POIs) for subsequent poly-ubiquitination and proteasomal degradation.[7] The efficacy of this approach hinges on efficient ternary complex formation between the PROTAC, POI, and E3 ligase.[8, 9] This not only requires sufficiently high affinity binders for both the POI and E3 ligase but also optimized linker geometry; all of which is difficult to simultaneously optimize in classical "ligand-first" PROTAC synthesis campaigns.[1, 5, 10] Thus, despite the promise of TPD, the development of novel PROTACs remains a significant challenge and has been met with limited success. Only a handful of POI classes with well-established POI ligands, .[9-12] such as kinases[13, 14] and BET[15, 16] proteins, have been successfully degraded

Mass spectrometry (MS)-based chemoproteomics has become an invaluable tool in chemical biology, wherein chemical probes enable the functional characterization of individual proteins within complex proteomes.[17] Key advances have established efficient methods for proteome-wide mapping and ligand screening in native biological systems,[18-26] aiding in the development of novel inhibitors and E3 ligase recruiters[27, 28]. However, these methods have limited utility in PROTAC

discovery, as mere PROTAC binding to the POI does not guarantee proteasomal degradation. To address this limitation and expand the range of druggable proteins, we propose a strategy for *de novo* PROTAC discovery that features the synthesis of collections of target-agnostic covalent PROTAC probes and systematic, proteome-wide identification of their protein targets (target ID) via global proteomics. We believe that this PROTAC-centric approach is more effective than first identifying targets of ligands and then attempting to convert them into PROTAC probes,[29] which may not ultimately yield a working PROTAC. Moreover, covalent PROTACs have the potential to further enhance target diversity towards difficult therapeutic targets, resulting from the combined advantages of both traditional PROTACs and covalent inhibition.[1]

Global proteomics offers a streamlined protocol for observation of proteome-wide changes in abundance levels, which has been leveraged to identify degraded proteins.[30-32] It also enables visualization of diverse classes of proteins – including low molecular weight proteins incompatible with precipitation steps in enrichment-based proteomic workflows. Although extensive changes following compound treatment can be difficult to interpret, our two-part comparative approach identifies proteins selectively downregulated by our PROTAC versus the warhead and active linker-E3 ligase ligands alone. This allows us to better mimic non-productive PROTAC binding and filter out indirectly dysregulated proteins We demonstrate how our approach led to the discovery of a first-in-class, selective acrylamide-based degrader for metallothionein 2A (MT2A), an "undruggable" protein with high therapeutic relevance.

MTs are small, cysteine-rich proteins that chelate up to seven divalent cations to maintain numerous biological processes including zinc homeostasis and metal detoxification.[33] Their unique metal-binding properties also play critical roles in various pathophysiological processes, including cell proliferation,[34] metastasis,[35] and cell cycle arrest[36,37] Due to the lack of noteworthy chemical tools for MTs, research has primarily focused on the biophysical and structural characterization of metalation[38, 39] and correlative phenotypic studies using genetic knockdown[35, 40-45] (Figure 1, top). Using our first-in-class MT2A PROTAC, we demonstrate that MT2A degradation inhibits cancer cell migration and invasion through DIAPH3-dependent cytoskeletal remodeling (Figure 1, bottom).

In conclusion, the herein presented chemoproteomic method offers a rapid and efficient approach for *de novo* discovery of covalent PROTACs with minimal experimental optimization. We successfully apply our method to discover an MT2A-targeting PROTAC as a first-in-class chemical tool to study native MT-regulated cellular processes.

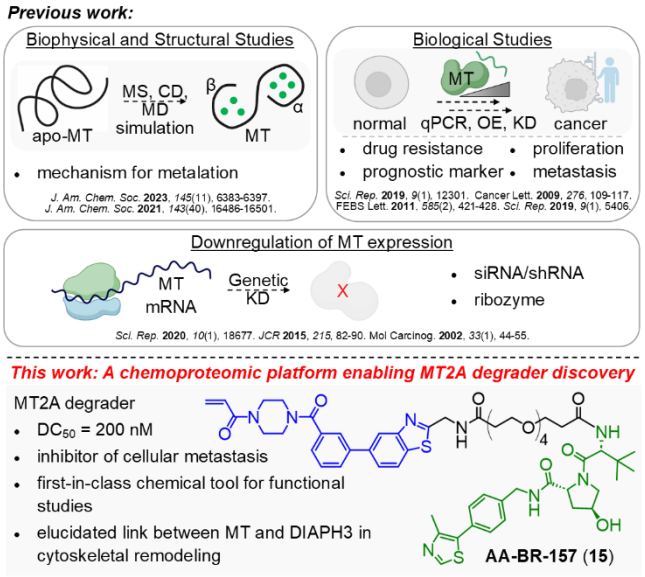

Figure 1. Previous studies into metallothionein family members (top) as well as our current work identifying a MT2A targeted degrader (bottom).

Results & discussion

Cysteines play diverse structural and functional roles in biology,[17] owing in part to the enhanced nucleophilicity of their side chain thiol. As a result, the cysteine thiol serves as an attractive target in inhibitor discovery[19, 46-50] and, more recently, in PROTAC development.[10, 27, 51] We synthesized a small collection of target-agnostic, cysteine-reactive PROTACs by joining the von Hippel Lindau (VHL) ligand with various acrylamides via a polyethylene glycol (PEG) linker. A full chemical and chemoproteomic characterization of this small collection of PROTAC probes will be reported by us in due course. We herein describe our two-component chemoproteomic method to rapidly identify the cellular targets of our *de novo* PROTAC probes (Figure 2A). Briefly, cells are treated with the PROTAC, or its constituent linker-E3 ligase recruiter or POI ligands alone and then subjected to MS-based global proteomics analysis. Treatment with the latter two control probes allows us to better filter out protein abundance changes due to the warhead or E3 ligase recruiter binding alone, thus increasing confidence in validating direct cellular targets of our degraders. We then show how our method led to the discovery of a first-in-class degrader and novel chemical tool for metallothionein 2A (MT2A), a small "undruggable" protein with high therapeutic importance.

Synthesis of PROTAC 10 and Target Identification. We initiated our synthetic studies with the preparation of acrylamide warhead **7**. Briefly, piperazine **3** and benzothiazole **6** were independently generated via peptide coupling and palladium-catalyzed cyclocondensation, respectively (Figure 2B). These fragments were then subjected to Suzuki-Miyaura cross-coupling followed by coupling of the piperazine with acryloyl chloride to obtain electrophilic acrylamide **7**. Treatment of **7** with TFA yielded the unprotected amine **8**, which was then used to access PROTAC **10** via a HATU- mediated peptide coupling with PEG6-appended VHL E3 ligase ligand **9**.

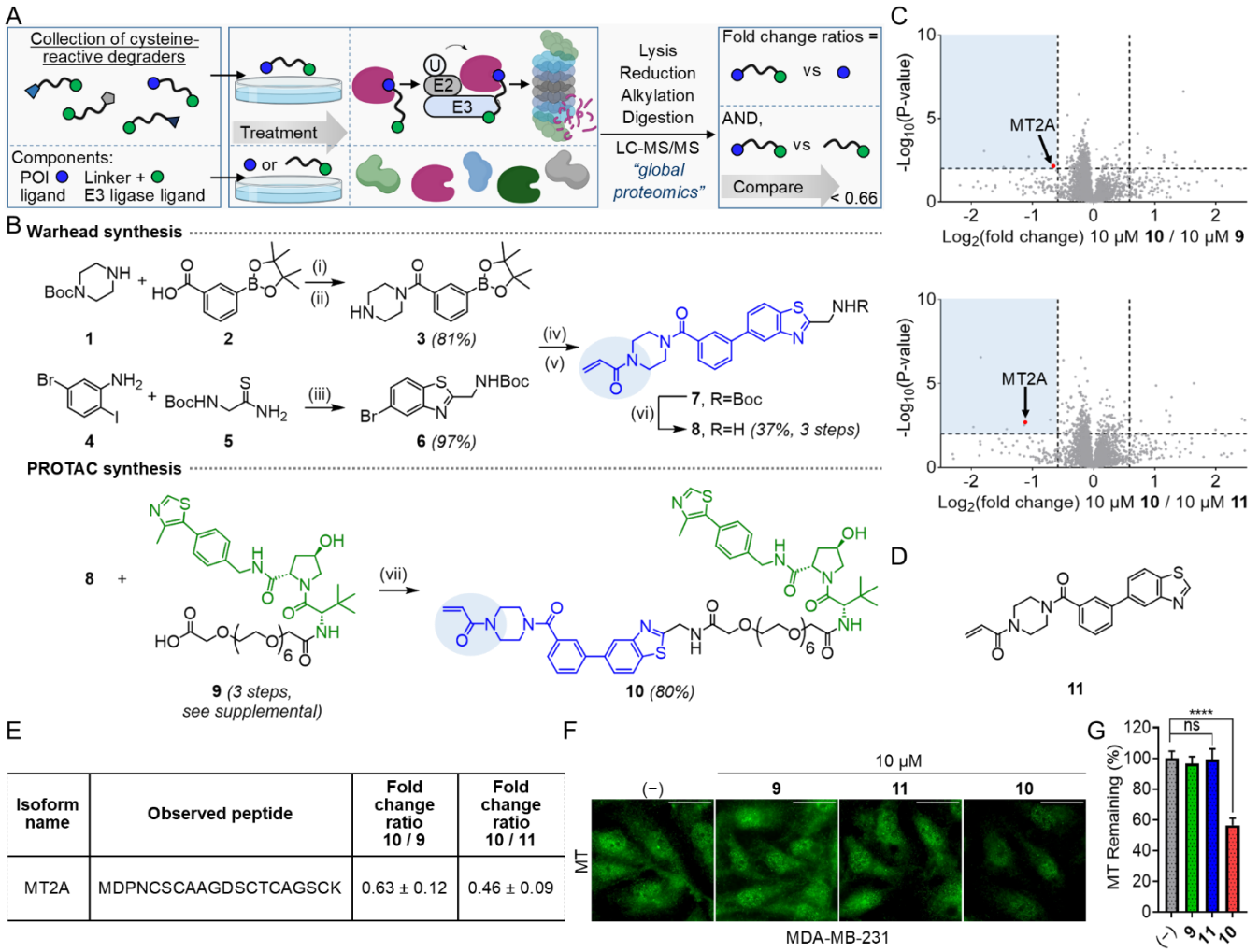

Isoform name	Observed peptide	Fold change ratio 10 / 9	Fold change ratio 10 / 11
MT2A	MDPNCSCAAGDSCTCAGSCK	0.63 ± 0.12	0.46 ± 0.09

Figure 2. Identification of a targeted degrader for metallothionein-2A. A) Schematic workflow of our LC-MS/MS-based PROTAC discovery approach. B) Synthesis of PROTAC **10**. Reaction conditions: (i) **1** (1.2 equiv), **2** (1 equiv), EDC (1.1 equiv), HOBt (1.1 equiv), and DIPEA (3.0 equiv) in DCM, rt, 12 h; (ii) TFA (14.5 equiv) in DCM, rt, 2 h; (iii) CuO (1.0 equiv), dppf (0.2 equiv), and $Pd_2(dba)_3$ (0.1 equiv) in degassed DMF, 60°C, 12 h; (iv) **3** (1.5 equiv), $Pd(dppf)Cl_2$ (0.1 eq), and Cs_2CO_3 (4.5 eq) in degassed 1,4-dioxane/H_2O, 100°C, 12 h; (v) acryloyl chloride (1.2 equiv) and TEA (3.0 equiv) in DCM, 0°C to rt, 3 h; (vi) TFA (14.5 equiv) in DCM, rt, 2 h; (vii) **8** (1.2 equiv), HATU (1.5 equiv), and DIPEA in DMF, rt, 2 h. C) Volcano plots showing proteome-wide changes in protein levels identified using the general workflow presented in (A) comparing treatment of MDA-MB-231 cells with 10 μM **10** versus 10 μM **9** (top) and 10 μM **11** (bottom) for 24 h (n = 6, 2 biological x 3 technical). Blue regions highlight the proteins selectively downregulated by PROTAC **10**. Dotted lines represent the following thresholds: $-Log_{10}$(P-value) = 2 and Log_2(fold change) = -0.6 and 0.6. D) Chemical structure of POI ligand acryloylpiperazine **11**. E) Table of calculated fold change ratios for identified MT2A peptide. Shown as average fold change ± SDs. F) Immunofluorescence microscopy images and G) quantification of MT staining in MDA-MB-231 cells treated with either DMSO, or 10 μM **9**, **10**, or **11** for 24 h. White bars indicate 30 μm. Shown as fold changes to DMSO-treated cells ± SDs (n = 9). ****$p < 0.0001$ by unpaired Student's t-test; ns indicates $p > 0.05$.

The cellular targets of PROTAC **10** were then identified using our *de novo* discovery platform. Briefly, triple negative breast cancer (TNBC) MDA-MB-231 cells were treated with 10 μM **10, 9**, or **11** for 24 h followed by lysis, reduction, alkylation, digestion, and liquid chromatography-tandem mass spectrometry (LC-MS/MS)-based global proteomics. Comparative analyses revealed a small subset of proteins that exhibited significant downregulation (fold change ratio < 0.66) upon treatment with PROTAC **10** but not with the linker-appended VHL ligand **9** or warhead **11** (Figure 2C, D and Table S1). Owing to our interest in zinc-cysteine interactions,[52] MTs emerged as intriguing potential targets of **10** for their prominent but understudied roles in zinc homeostasis and regulation of vital cellular processes (e.g., cell proliferation,[36] metastasis[35], and

apoptosis[53, 54]).[37] Human MTs are categorized into four sub-families (MT1-4), of which only MT1s and MT2 are ubiquitously expressed across different tissue types.[37] Among the detected MT isoforms, only MT2A exhibited fold change ratios below our set thresholds for both **10** versus **9** (0.63) and **10** versus **11** (0.46) (Figure 2E).

We were particularly enthusiastic about MT2A considering reports indicating that this protein is the most abundant and biologically significant MT isoform across numerous cell lines with key roles in the regulation of TNBC metastasis, among others.[35, 55-58] To preliminarily assess whether PROTAC **10** specifically downregulates endogenous MTs, we treated MDA-MB-231 cells with DMSO, **9**, **10**, or **11** and visualized MT levels by immunofluorescence microscopy using a non-specific MT antibody due to the limited availability of commercial isoform-specific antibodies. As anticipated, no changes in MT levels were observed upon treatment with DMSO, **9**, and **11**, whereas an ~2-fold decrease was observed upon treatment with **10** (Figures 2F, G and Figure S1).

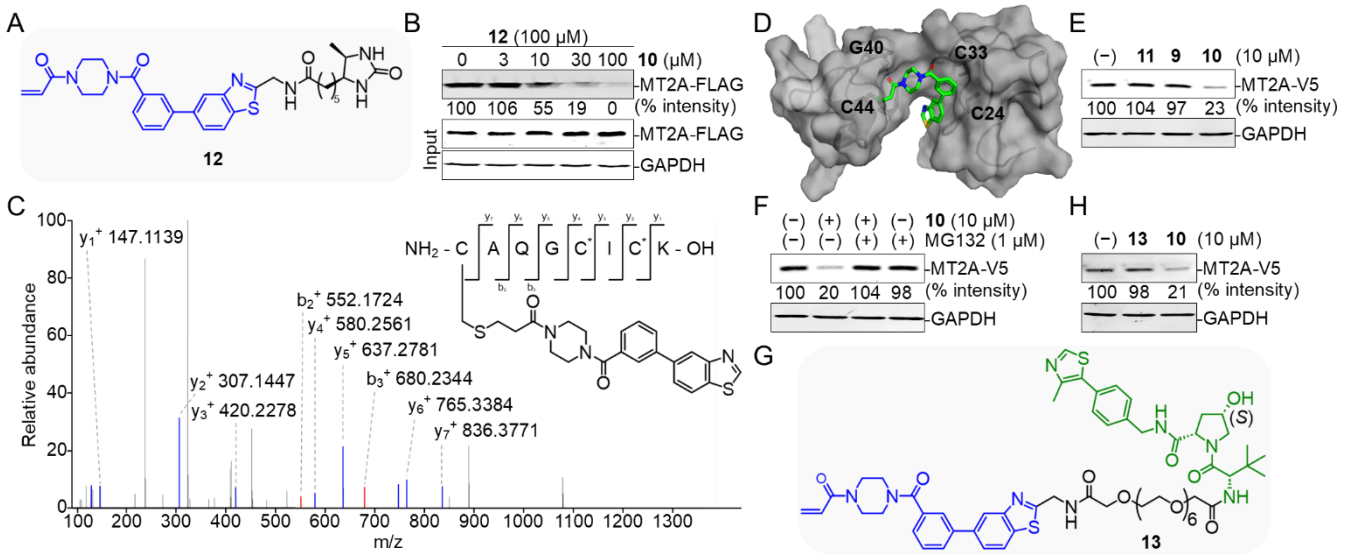

Figure 3. Validating **10** as a targeted degrader of MT2A. A) Chemical structure of desthiobiotin-functionalized probe **12**. B) Chemical competitive pull-down of overexpressed MT2A-FLAG from HEK293T lysates pre-treated with various concentrations of PROTAC **10** for 2 h at 37°C followed by treatment with 100 μM desthiobiotin probe **12** for 2 h at 37°C. Proteins were enriched via streptavidin agarose beads, eluted, and visualized by Western blot with FLAG antibody. Eluted proteins are shown on top, and the corresponding input controls are below. C) Annotated MS/MS spectrum of modified C44 on His_6-MT2A with POI ligand acryloylpiperazine **11**. * indicates cysteine carbamidomethylation. D) Covalent docking of POI ligand acryloylpiperazine **1** onto MT2A at C44. Residues critical for ligand binding are highlighted in black. Western blotting analysis of MT2A-V5 expression in MT2A OE cells treated for 24 h with E) DMSO, or 10 μM **9**, **10**, or **11**; or F) DMSO, 10 μM **10**, 1 μM (*S*)-MG132 (18 h), or pre-treatment with 10 μM **10** (6 h) followed by co-treatment with 1 μM (*S*)-MG132 (18 h). Western blot membranes were probed for V5. G) Chemical structure of inactive epimeric PROTAC **13** and H) subsequent Western blotting analysis of MT2A-V5 expression in MT2A OE cells treated for 24 h with DMSO, or 10 μM inactive PROTAC **13** or active PROTAC **10**.

PROTAC 10 Binds and Degrades MT2A. Following identification of MT2A, we then proceeded to validate this protein as a direct target of **10** using a competitive pull-down assay and protein adduct analysis by proteomics. Overexpressed MT2A-FLAG lysate was treated with increasing concentrations of **10** for 2 h at 37°C, followed by treatment with 100 μM probe **12**, a desthiobiotin-functionalized derivative of ligand **11** (Figure 3A). The proteins were then precipitated, enriched over streptavidin beads, eluted, and visualized by Western blot. Excitingly, we observed not only enrichment of MT2A by **12** but also competition by PROTAC **10** in a concentration-dependent manner, thus establishing target engagement with low micromolar binding affinity (Figure 3B and Figure S2A). To further investigate the interaction between ligand **11** and MT2A, we pre-treated purified His_6-MT2A with either PBS or excess $ZnCl_2$ for metal saturation prior to the addition of **11** and LC-MS/MS analysis of the cysteine binding site. The cysteine-**11** adduct was observed on conserved C44 within the α-domain for both conditions, suggesting our PROTAC binds MT2A regardless of its metalation status (Figure 3C and Figure S3). Subsequent Schrödinger CovDoc analyses indicated that ligand **11** fits along the metal binding site of the α-domain and forms a hydrogen bond with G40 in the β-domain (Figure 3D). Importantly, our docking results indicate that ligand binding disrupts metal coordination within both domains through interactions with key metal coordinating residues C24, C29, and C33.

We next sought to determine whether **10** downregulates MT2A through *bona fide* targeted proteasomal degradation. We first generated stable MT2A-V5 overexpressing MDA-MB-231 (MT2A OE) cells via lentiviral transduction and re-confirmed MT2A downregulation via Western blot (Figure 3E and Figure S2B). We then investigated proteasomal dependence of this downregulation by pre-treating MT2A OE cells with 10 μM **10** for 6 h and then co-treating with 1 μM proteasomal inhibitor (*S*)-MG132 for 18 h. Indeed, MT2A levels were rescued in co-treated cells, indicating that the 80% decrease observed upon treatment with **10** occurs through proteasomal degradation (Figure 3F). To ensure the observed decrease in MT2A was dependent on VHL E3 ubiquitin ligase recruitment, we synthesized the inactive epimer of **10** featuring inverted stereochemistry of the hydroxyproline moiety of the VHL ligand (*R*→*S*, inactive PROTAC **13**) (Figure 3G). As expected, no

effect on MT2A levels was observed upon treatment with 10 μM **13** (Figure 3H). Collectively, our results confirm that **10** is a first-in-class targeted degrader of MT2A with low micromolar *in vitro* binding affinity.

Encouraged by these results, we then proceeded to quantify MT2A degradation by **10**. To determine the optimal treatment duration, MT2A OE cells were incubated with 10 μM **10** for various amounts of time prior to measuring MT2A levels by Western blot. We observed a half-maximal degradation (D_{50}) at 17.3 h and maximum degradation after 24 h (Figure S4). We then treated MT2A OE cells with various concentrations of **10** for 24 h to determine the potency of degradation. Indeed, we observed a dose-dependent decrease in MT2A expression with a half-maximal degradation concentration (DC_{50}) of 6.5 μM and maximal level of degradation (D_{max}) of ~70% (Figures 3A, 3B). Some recovery of protein signal was observed at 30 μM due to unproductive ternary complex formation, a phenomenon that has been reported for other covalent PROTACs at high concentrations (i.e., the Hook effect).[10]

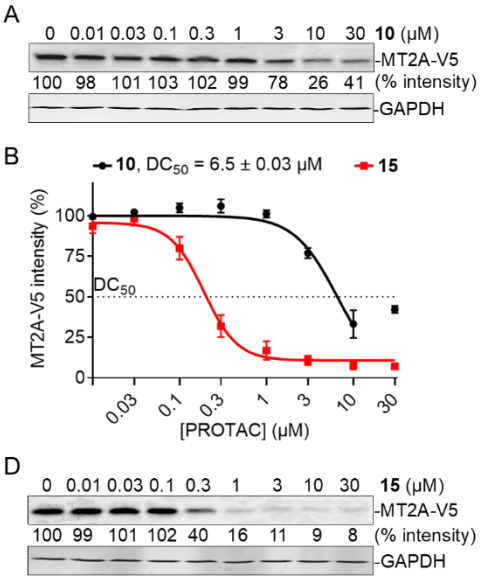

C

PROTAC	Linker (R^1=POI ligand; R^2=VHL ligand)	Length	DC_{50} (μM)	D_{MAX} (%)
14	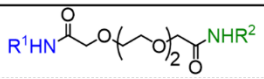	11	2.82 ± 0.05	76.6 ± 4.5
15	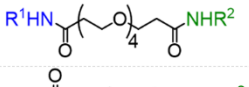	16	0.19 ± 0.03	92.2 ± 1.9
16	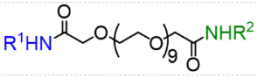	32	3.00 ± 0.06	70.7 ± 4.1
17	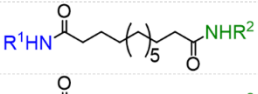	12	N.D.	44.1 ± 3.2
18	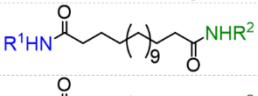	16	N.D.	36.4 ± 3.3
19	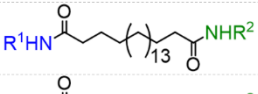	20	N.D.	48.2 ± 7.3
20	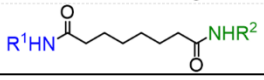	8	N.D.	36.9 ± 2.2

Figure 4. Optimization towards potent PROTAC **AA-BR-157** (**15**). A) Western blot of concentration-dependent MT2A degradation in MT2A OE cells treated with **10** for 24 h to determine its half maximal degradation concentration (DC_{50}). B) Quantification of MT2A degradation upon treatment **10** or **15**, corresponding to the Western blots in (A) and (D), respectively. Degradation at 30 μM **10** was not included in the fitting due to the Hook effect. Shown as normalized values ± SDs (n = 3). Western blot membrane probed for V5. C) Table of DC_{50} and D_{max} values for MT2A OE cells treated with PEG- or alkyl- linker containing PROTACs **14**-**20** for 24 h. Degradation at 30 μM **14** was not included in fitting due to Hook effect. Shown as normalized values ± SDs (n = 3). D) Western blot of concentration-dependent MT2A degradation in MT2A OE cells treated with **15** for 24 h.

Next, we sought to improve the degradation potency towards MT2A by optimizing the linker length and composition.[59, 60] We synthesized three derivatives with varied PEG linker lengths (PEG2, 4, and 9; compounds **14-16**); the corresponding alkyl derivatives of PROTACs **11**, **14**, and **15** (C12, 16, and 20; compounds **17-19**); and a shorter C8 alkyl derivative. MT2A OE cells were then treated with increasing concentrations of **14-20** for 24 h prior to measuring MT2A levels via Western blot. We observed a dose-dependent decrease in MT2A levels with all PROTACs, but interestingly, there was no obvious trend between linker length and degradation (Figure 4C and Figure S5). There was, however, significantly higher degradation observed with all the PEG-containing PROTACs compared to those with alkyl linkers. Gratifyingly, the PEG4-based PROTAC (**15**, **AA-BR-157**) exhibited an ~35-fold higher potency than **10** with a DC_{50} value of 200 nM and sustained D_{max} of 90% starting at ~1 μM (D_{50} = 14.6 h; Figure 3B, C, D and Figure S6). No protein recovery was observed at higher concentrations, suggesting a broad therapeutic window for maximal degradation. Covalent PROTACs are historically criticized for their non-catalytic mechanism of action, which was thought to reduce potency.[61, 62] While difficult to compare directly due to differences in protein targets, the potency of **AA-BR-157** is on the same order of magnitude as that of many previously reported high-efficiency PROTACs.[10, 63, 64]

Moreover, MS-based global proteomic analyses also revealed that **AA-BR-157** exhibits notable selectivity in complex proteomes. For this, MDA-MB-231 cells were treated with **AA-BR-157**, the PEG4-linked VHL E3 ligase ligand **15a**, or the warhead **11** (all at 10 μM) for 24 h, followed by lysis, reduction, alkylation, digestion, LC-MS/MS analysis, and data processing using MaxQuant. Gratifyingly, among the 4,220 quantified proteins, MT2A was the only protein downregulated by **AA-BR-157** but not by either control compound (Figure S7 and Table S2). Altogether, our results highlight the potential of **AA-BR-157** as a first-in-class degrader of MT2A.

AA-BR-157 Inhibits Cellular Migration via DIAPH3-dependent Cytoskeletal Remodeling. With our optimized PROTAC in hand, we then sought to investigate its potential as a research tool to better understand the role that MTs play in driving cancer metastasis. Isoform-specific MT overexpression has been shown to augment cellular migration and invasion across several cancer cell lines, though precise mechanisms are unknown.[35, 56, 65] To this end, we first performed transwell migration assays using metastatic TNBC MDA-MB-231 and glioblastoma U-87 MG cells. Cells were treated with DMSO, MT siRNA as a

genetic control, or increasing concentrations of **AA-BR-157** and allowed to migrate across the transwell chamber for 24 h. Excitingly, we observed a concentration-dependent decrease in cellular migration, with a maximal decrease greater than 60% following treatment with 10 μM **AA-BR-157** and MT siRNA across cell lines (Figures 5A and S8, and Table S3). We then excluded the possibility that latent PROTAC cytotoxicity was responsible for this decrease, as no cell death was observed upon exposure to **AA-BR-157** in a WST-1 assay (Figure 5B). Further, we confirmed that our PROTAC also inhibits MDA-MB-231 cellular invasion through Matrigel using the transwell assay (Figures 5C, 5D).

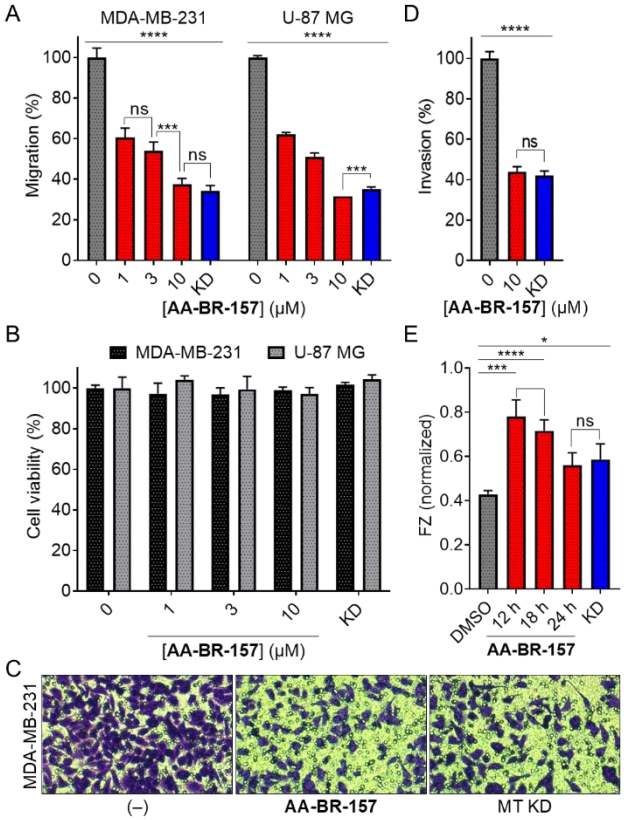

Figure 5. AA-BR-157-mediated degradation of MT2A inhibits cellular metastasis and increases intracellular zinc levels. A) Quantification of TNBC MDA-MB-231 and glioblastoma U-87 MG cells that migrated during a 24 h transwell assay following treatment with DMSO, the indicated concentration of **AA-BR-157**, or MT siRNA (KD; treated for 48 h) for 24 h. Shown as normalized percentages ± SDs (n = 3). B) WST-1 assay measuring the toxicity of **AA-BR-157** (24 h) and MT siRNA knockdown (48 h) in MDA-MB-231 (black) and U-87 MG (grey) cells. Cells were incubated with WST-1 (5%) for 1 h. Shown as normalized values ± SDs (n = 3). C) Crystal violet images and D) quantification of MDA-MB-231 cells that invaded during a 24 h transwell assay following treatment with DMSO, 10 μM **AA-BR-157**, or MT siRNA (KD; treated for 48 h) for 24 h. Shown as normalized percentages ± SDs (n = 3). E) Fluorescence spectroscopy quantification of intracellular zinc levels in MDA-MB-231 cells using 2 μM FZ-3AM. Cells were pre-treated with DMSO (24 h), 10 μM **AA-BR-157**, or MT siRNA (KD; 48 h) for the indicated time lengths, prior to incubation with FZ-3AM for 30 min and then PBS for 1 h to allow for hydrolysis and activation of FZ-3AM. Fluorescence intensity was normalized using a WST-1 cytotoxicity assay. Shown as normalized fluorescence ± SDs (n = 6). *p < 0.005, ***p < 0.0005, ****p < 0.0001 by unpaired Student's t-test; ns indicates p > 0.05.

To explore the mechanistic link between MT2A degradation and suppression of MDA-MB-231 cell migration, we first investigated the effect on zinc homeostasis. All cells regulate a small pool of labile zinc (Zn^{2+}), which readily interacts with cysteines, as well as histidines, aspartic acids, and glutamic acids, to affect cellular processes, such as cell cycle progression.[52, 66] Since each MT maximally coordinates seven Zn^{2+} that are excluded from the labile zinc pool, we hypothesized that PROTAC-mediated degradation of MT2A would cause a measurable increase in intracellular Zn^{2+} and broadly influence cellular functions.[57, 66-69] To probe our hypothesis, we first quantified intracellular Zn^{2+} levels upon time-dependent treatments with **AA-BR-157** and MT siRNA using zinc-specific FluoZin-3AM dye and fluorescence spectroscopy. As expected, Zn^{2+} levels were markedly increased following 12 and 18 h treatment with **AA-BR-157** but tapered at 24 h, likely due to gradual compensation through other zinc-binding proteins (Figure 5E). Conversely, only a modest increase in Zn^{2+} levels was observed upon MT siRNA knockdown, which we attribute to the longer treatment time required to observe knockdown (48 h) versus degradation.

Intrigued by these results, we employed comparative global proteomics to investigate the proteome-wide effects of elevated Zn^{2+} levels caused by the decrease in MT2A levels. MDA-MB-231 cells were treated with DMSO, 10 μM **AA-BR-157**, or MT siRNA and subjected to LC-MS/MS analysis to identify commonly up- or downregulated proteins (Figure 6A and Table S4). Among these commonly dysregulated proteins, protein diaphanous homolog 3 (DIAPH3) emerged as an interesting target due to its established pro-cancerous role in cellular migration and cytoskeletal architecture (Figure 6B).[70, 71] DIAPH3 is an

actin nucleation and elongation factor required for assembly of actin cables and stress fibers.[70] Furthermore, Jang and coworkers disclosed a link between MT1E, matrix metalloproteinase (MMP)-9 expression, and/or cytoskeletal remodeling during glioma metastasis.[65] Suspecting a similar relationship, we validated the downregulation of DIAPH3 in MDA-MB-231 cells following treatment with various concentrations of **AA-BR-157** and MT siRNA via Western blot. An ~50% decrease in DIAPH3 levels was observed following treatment with both **AA-BR-157** and MT siRNA (Figure 6C).

We then leveraged Deep Structured Illumination Microscopy (DeepSIM) super-resolution imaging to investigate the effects of MT and DIAPH3 downregulation on MDA-MB-231 cytoskeletal morphology. Cell motility requires dynamic polarization in the direction of movement, which is easily observed in the DMSO-treated cells (Figure 6D and Figure S9).[72] Cells treated with 10 μM **AA-BR-157** and both MT and DIAPH3 siRNAs, however, exhibited a strongly rounded (unpolarized) shape, indicating a loss of actin cables and migratory potential compared to the DMSO-treated cells. As expected, a similar effect was also observed with the remaining cytoskeletal components – intermediate filaments (vimentin) and microtubules (tubulin). Vimentin reorganized from a strong perinuclear localization with tail-like projections in migrating DMSO-treated cells to a dispersed cytosolic staining in the non-migrating cells,[73, 74] whereas tubulin was broadly dispersed throughout the cytosol. Importantly, DIAPH3 knockdown control cells recapitulated the morphology of MT-downregulated cells (Figure S10), suggesting that MTs may regulate cellular migration through DIAPH3 downregulation and cytoskeletal remodeling.

Collectively, these results demonstrate that **AA-BR-157** is an excellent chemical tool to study MT2A at the cellular level, thus addressing a longstanding challenge associated with the limited availability of research tools to probe native MT biology.

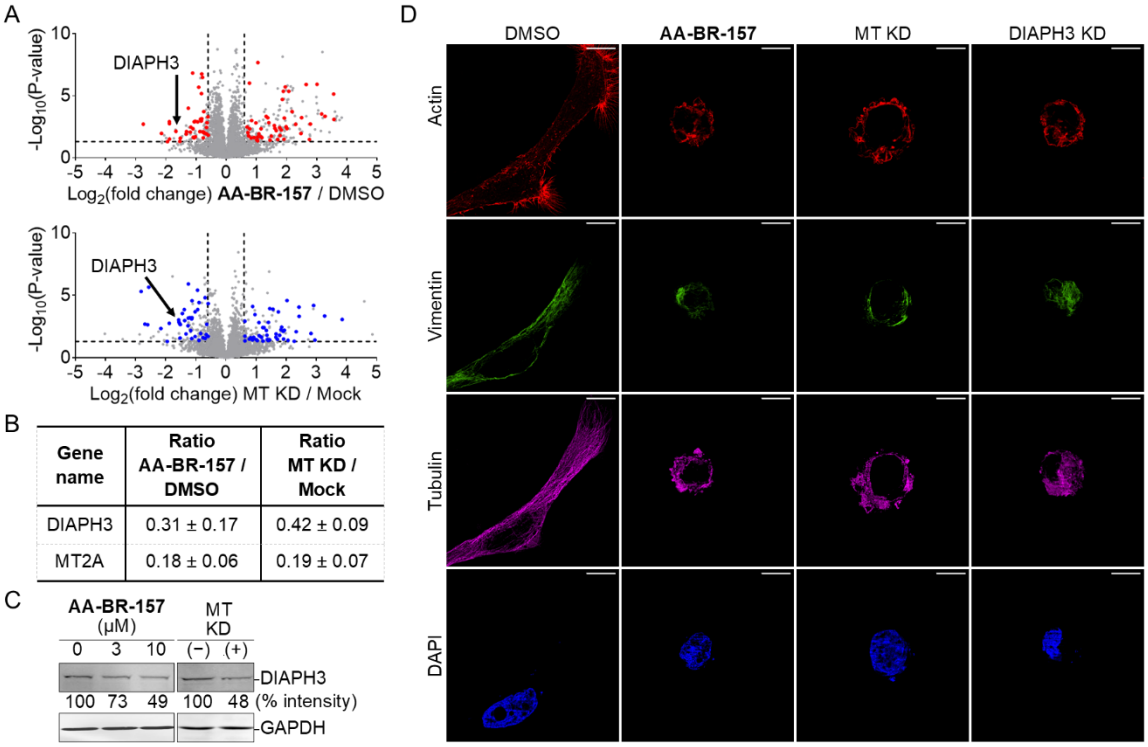

Figure 6. AA-BR-157-mediated degradation of MT2A inhibits cellular metastasis through DIAPH3-dependent cytoskeletal remodeling. A) Volcano plots showing global protein expression changes in MDA-MB-231 cells treated with either 10 μM **AA-BR-157** versus DMSO for 24 h (top), or MT siRNA versus Mock for 48 h (bottom). Colored dots represent proteins commonly down- or up-regulated by both **AA-BR-157** and MT siRNA treatments (n = 6, 2 biological x 3 technical). Dotted lines represent the following thresholds: $-\text{Log}_{10}$(P-value) = 1.3 and Log_2(fold change) = -0.6 and 0.6. B) Table of downregulation ratios for MT2A and DIAPH3, a protein linked to cellular migration. Shown as average fold change ± SDs. C) Confirmation by Western blot analysis of DIAPH3 expression in MDA-MB-231 cells following treatment with DMSO, the indicated concentrations of **AA-BR-157,** or MT siRNA (48 h) for 24 h, unless otherwise noted. D) DeepSIM super-resolution microscopy images of the cytoskeleton components showing actin (red), vimentin (green), tubulin (purple), and DAPI (blue) immunofluorescence staining of MDA-MB-231 cells treated with either DMSO or 10 μM **AA-BR-157** for 24 h; or MT siRNA or DIAPH3 siRNA for 48 h. White bars indicate 10 μm.

Conclusions

In summary, we presented our chemoproteomics-enabled PROTAC discovery method, which facilitates the elucidation of degraders of disease-implicated proteins currently considered undruggable. Classical enrichment-based target ID methods are highly beneficial for inhibitor discovery, but binding alone is insufficient for identifying functional targeted degraders. As a result, PROTAC development has predominantly relied on the use of previously established high affinity ligands and requires extensive optimizations to degrade the intended target, which is not only time consuming but fails to expand the druggable proteome. We show that our global proteomics method offers an excellent alternative for novel PROTAC discovery.

The output of this method illuminates changes in protein levels across the proteome to identify functional degraders with minimal optimization required. Furthermore, our method features a PROTAC versus ligand comparison step that allows for stringent and rapid identification of proteins that are degraded rather than just downregulated following ligand binding. Without this crucial step, global proteomics-based target ID may require extensive pathway analyses using predetermined phenotypes to deconvolute truly degraded hit proteins from unrelated transcriptional downregulation.

We showed that our cysteine-reactive PROTACs provide a strong foundation for selective degradation of challenging therapeutic targets for which no high-affinity inhibitors are available. Herein, we presented the rapid development and in-depth evaluation of our acrylamide- and VHL-based PROTAC as a targeted degrader for MT2A, a protein with strong therapeutic potential but no reported small molecule modulators. This is likely due to its lack of clear binding pockets and small size (~6 kDa), enabling it to elude detection in enrichment-based ligand screening. Altogether, identification of an MT2A targeted degrader emphasizes the ability of our method to identify degraders of challenging therapeutic targets – like small proteins with minimal structural domains for inhibitor binding. Importantly, unlike many chemoproteomic fragment discovery methods,[26, 75] which are often limited to one particular class of small molecule ligands, our method should, in principle, be compatible with any class of small molecules.

We further demonstrated that our lead PROTAC **10** degrades MT2A through engagement with C44 via the *bona fide* proteasomal degradation mechanism. With only minimal optimization, we obtained a more potent degrader **AA-BR-157** (DC_{50} = 200 nM; D_{max} = 90%). Collectively, our discovery of an MT2A-targeting PROTAC offers a first-in-class chemical tool to natively study MT-regulated processes, whereas current methods are limited to genetic knockdown[55, 76-78] and/or correlative gene expression or purified protein studies.[53, 79-81]

Aberrant MT overexpression has been linked to the increased metastatic potential of several cancers, including breast cancer and glioblastoma.[35, 56, 65] Previous reports by Jang and coworkers suggested that MTs may regulate cellular migration through inhibition of MMP-9 and/or through cytoskeletal remodeling, though no cytoskeletal remodeling proteins were identified.[65] Our subsequent biochemical experiments show **AA-BR-157** not only decreases cellular migration and invasion of aggressive cancer cell lines, but also downregulates DIAPH3, a positive regulator of actin and cell motility,[70, 71] and strongly inhibits cell polarization.

Further work is needed to better understand the regulatory relationship between MT2A and DIAPH3, but it is plausible that MT2A regulates a zinc-binding transcription factor responsible for DIAPH3 synthesis.[33] MTs have already been shown to interact with a myriad of proteins, such as transcription factors (e.g., NF-κB[82] and TFIIIA[69]), metalloproteins (e.g., MMP-9[35] and Cu/Zn SOD[83]), and endocytic receptors (e.g., low-density lipoprotein receptors[84]), many of which interact during direct zinc exchange.[33] Given that MT overexpression is implicated in several pro-cancerous pathways (e.g., metastasis[35, 56, 65], drug resistance[57, 77]) across several cancer types, we believe that **AA-BR-157** represents an excellent starting point for the development of more potent MT2A-targeting degraders with broad clinical anti-cancer potential. Our efforts are currently being devoted to further our mechanistic understanding of the biochemical consequences of MT2A degradation and to investigate the impact of MT2A degradation on cancer metastasis *in vivo*.

Associated content

Supporting Information. The Supporting Information is available free of charge at XXXX.

Experimental procedures, supporting figures, chemical synthesis, and spectra (PDF).

Supporting Proteomic Tables (Excel).

Author information

Corresponding Author

* Alexander Adibekian- Departments of Chemistry, Pharmaceutical Sciences, and Biochemistry and Molecular Genetics, University of Illinois Chicago, University of Illinois Cancer Center, Chicago, IL 60607, United States; ORCID 0000-0001-6453-0244; Email: aadibeki@uic.edu

Present Addresses

†Brendan Dwyer- Department of Chemical and Systems Biology, Chem-H and Stanford Cancer Institute, Standford School of Medicine, Stanford University, Stanford, CA 94305, United States

Author Contributions

A.A. conceived the study and supervised the work. B.R., D.P., and A.A. were involved in the design and execution of the synthesis. B.R., D.P., D.A., B.D., and A.A. designed and performed biological studies. B.R., N.R., Y.H., and A.A. designed and performed the DeepSIM fluorescence microscopy experiments. B.R. and A.A. wrote the manuscript, and all authors reviewed and edited the manuscript.

Funding Sources

This work was supported by the National Institutes of Health grant RO1GM145886 (to A.A.), Enveda Biosciences sponsored research grant (to A.A.), and UIC LAS Endowed Professorship (to A.A.). B.R. was supported by the David C. Fairchild Endowed Fellowship and the NSF Graduate Research Fellowship.

Notes

The authors declare no competing financial interest.

References

(1) Gabizon, R.; London, N. The rise of covalent proteolysis targeting chimeras. *Curr Opin Chem Biol* **2021**, *62*, 24-33. DOI: 10.1016/j.cbpa.2020.12.003.
(2) Li, X.; Song, Y. Proteolysis-targeting chimera (PROTAC) for targeted protein degradation and cancer therapy. *J Hematol Oncol* **2020**, *13* (1), 50. DOI: 10.1186/s13045-020-00885-3.
(3) Samarasinghe, K. T. G.; Crews, C. M. Targeted protein degradation: A promise for undruggable proteins. *Cell Chem Biol* **2021**, *28* (7), 934-951. DOI: 10.1016/j.chembiol.2021.04.011.
(4) Burslem, G. M.; Crews, C. M. Proteolysis-Targeting Chimeras as Therapeutics and Tools for Biological Discovery. *Cell* **2020**, *181* (1), 102-114. DOI: 10.1016/j.cell.2019.11.031.
(5) Bondeson, D. P.; Smith, B. E.; Burslem, G. M.; Buhimschi, A. D.; Hines, J.; Jaime-Figueroa, S.; Wang, J.; Hamman, B. D.; Ishchenko, A.; Crews, C. M. Lessons in PROTAC Design from Selective Degradation with a Promiscuous Warhead. *Cell Chem Biol* **2018**, *25* (1), 78-87 e75. DOI: 10.1016/j.chembiol.2017.09.010.
(6) Burslem, G. M.; Smith, B. E.; Lai, A. C.; Jaime-Figueroa, S.; McQuaid, D. C.; Bondeson, D. P.; Toure, M.; Dong, H. Q.; Qian, Y. M.; Wang, J.; et al. The Advantages of Targeted Protein Degradation Over Inhibition: An RTK Case Study. *Cell Chemical Biology* **2018**, *25* (1), 67-77. DOI: 10.1016/j.chembiol.2017.09.009.
(7) Spradlin, J. N.; Zhang, E.; Nomura, D. K. Reimagining Druggability Using Chemoproteomic Platforms. *Acc Chem Res* **2021**, *54* (7), 1801-1813. DOI: 10.1021/acs.accounts.1c00065.
(8) Pettersson, M.; Crews, C. M. PROteolysis TArgeting Chimeras (PROTACs) - Past, present and future. *Drug Discov Today Technol* **2019**, *31*, 15-27. DOI: 10.1016/j.ddtec.2019.01.002.
(9) Xue, G.; Chen, J. H.; Liu, L. H.; Zhou, D. L.; Zuo, Y. Y.; Fu, T. C.; Pan, Z. Y. Protein degradation through covalent inhibitor-based PROTACs. *Chem Commun* **2020**, *56* (10), 1521-1524. DOI: 10.1039/c9cc08238g.
(10) Gabizon, R.; Shraga, A.; Gehrtz, P.; Livnah, E.; Shorer, Y.; Gurwicz, N.; Avram, L.; Unger, T.; Aharoni, H.; Albeck, S.; et al. Efficient Targeted Degradation via Reversible and Irreversible Covalent PROTACs. *J Am Chem Soc* **2020**, *142* (27), 11734-11742. DOI: 10.1021/jacs.9b13907.
(11) Scheepstra, M.; Hekking, K. F. W.; van Hijfte, L.; Folmer, R. H. A. Bivalent Ligands for Protein Degradation in Drug Discovery. *Computational and Structural Biotechnology Journal* **2019**, *17*, 160-176. DOI: https://doi.org/10.1016/j.csbj.2019.01.006.
(12) Han, X.; Zhao, L.; Xiang, W.; Qin, C.; Miao, B.; Xu, T.; Wang, M.; Yang, C. Y.; Chinnaswamy, K.; Stuckey, J.; et al. Discovery of Highly Potent and Efficient PROTAC Degraders of Androgen Receptor (AR) by Employing Weak Binding Affinity VHL E3 Ligase Ligands. *J Med Chem* **2019**, *62* (24), 11218-11231. DOI: 10.1021/acs.jmedchem.9b01393.
(13) Lai, A. C.; Toure, M.; Hellerschmied, D.; Salami, J.; Jaime-Figueroa, S.; Ko, E.; Hines, J.; Crews, C. M. Modular PROTAC Design for the Degradation of Oncogenic BCR-ABL. *Angew Chem Int Ed Engl* **2016**, *55* (2), 807-810. DOI: 10.1002/anie.201507634.
(14) Zhang, C.; Han, X. R.; Yang, X.; Jiang, B.; Liu, J.; Xiong, Y.; Jin, J. Proteolysis Targeting Chimeras (PROTACs) of Anaplastic Lymphoma Kinase (ALK). *Eur J Med Chem* **2018**, *151*, 304-314. DOI: 10.1016/j.ejmech.2018.03.071.
(15) Zengerle, M.; Chan, K.-H.; Ciulli, A. Selective Small Molecule Induced Degradation of the BET Bromodomain Protein BRD4. *ACS Chemical Biology* **2015**, *10* (8), 1770-1777. DOI: 10.1021/acschembio.5b00216.
(16) Lu, J.; Qian, Y.; Altieri, M.; Dong, H.; Wang, J.; Raina, K.; Hines, J.; Winkler, James D.; Crew, Andrew P.; Coleman, K.; et al. Hijacking the E3 Ubiquitin Ligase Cereblon to Efficiently Target BRD4. *Chemistry & Biology* **2015**, *22* (6), 755-763. DOI: https://doi.org/10.1016/j.chembiol.2015.05.009.
(17) Hoch, D. G.; Abegg, D.; Adibekian, A. Cysteine-reactive probes and their use in chemical proteomics. *Chem Commun (Camb)* **2018**, *54* (36), 4501-4512. DOI: 10.1039/c8cc01485j.
(18) Backus, K. M.; Correia, B. E.; Lum, K. M.; Forli, S.; Horning, B. D.; Gonzalez-Paez, G. E.; Chatterjee, S.; Lanning, B. R.; Teijaro, J. R.; Olson, A. J.; et al. Proteome-wide covalent ligand discovery in native biological systems. *Nature* **2016**, *534* (7608), 570-574. DOI: 10.1038/nature18002.
(19) Abegg, D.; Tomanik, M.; Qiu, N.; Pechalrieu, D.; Shuster, A.; Commare, B.; Togni, A.; Herzon, S. B.; Adibekian, A. Chemoproteomic Profiling by Cysteine Fluoroalkylation Reveals Myrocin G as an Inhibitor of the Nonhomologous End Joining DNA Repair Pathway. *Journal of the American Chemical Society* **2021**, *143* (48), 20332-20342. DOI: 10.1021/jacs.1c09724.
(20) Browne, C. M.; Jiang, B.; Ficarro, S. B.; Doctor, Z. M.; Johnson, J. L.; Card, J. D.; Sivakumaren, S. C.; Alexander, W. M.; Yaron, T. M.; Murphy, C. J.; et al. A Chemoproteomic Strategy for Direct and Proteome-Wide Covalent Inhibitor Target-Site Identification. *J Am Chem Soc* **2019**, *141* (1), 191-203. DOI: 10.1021/jacs.8b07911.
(21) Weerapana, E.; Wang, C.; Simon, G. M.; Richter, F.; Khare, S.; Dillon, M. B.; Bachovchin, D. A.; Mowen, K.; Baker, D.; Cravatt, B. F. Quantitative reactivity profiling predicts functional cysteines in proteomes. *Nature* **2010**, *468* (7325), 790-795. DOI: 10.1038/nature09472.
(22) Vinogradova, E. V.; Zhang, X.; Remillard, D.; Lazar, D. C.; Suciu, R. M.; Wang, Y.; Bianco, G.; Yamashita, Y.; Crowley, V. M.; Schafroth, M. A.; et al. An Activity-Guided Map of Electrophile-Cysteine Interactions in Primary Human T Cells. *Cell* **2020**, *182* (4), 1009-1026.e1029. DOI: https://doi.org/10.1016/j.cell.2020.07.001.
(23) Abbasov, M. E.; Kavanagh, M. E.; Ichu, T.-A.; Lazear, M. R.; Tao, Y.; Crowley, V. M.; am Ende, C. W.; Hacker, S. M.; Ho, J.; Dix, M. M.; et al. A proteome-wide atlas of lysine-reactive chemistry. *Nature Chemistry* **2021**, *13* (11), 1081-1092. DOI: 10.1038/s41557-021-00765-4.

(24) Wright, M. H.; Tao, Y.; Drechsel, J.; Krysiak, J.; Chamni, S.; Weigert-Munoz, A.; Harvey, N. L.; Romo, D.; Sieber, S. A. Quantitative chemoproteomic profiling reveals multiple target interactions of spongiolactone derivatives in leukemia cells. *Chem Commun* **2017**, *53* (95), 12818-12821, 10.1039/C7CC04990K. DOI: 10.1039/C7CC04990K.
(25) Shannon, D. A.; Banerjee, R.; Webster, E. R.; Bak, D. W.; Wang, C.; Weerapana, E. Investigating the Proteome Reactivity and Selectivity of Aryl Halides. *Journal of the American Chemical Society* **2014**, *136* (9), 3330-3333. DOI: 10.1021/ja4116204.
(26) Parker, C. G.; Galmozzi, A.; Wang, Y.; Correia, B. E.; Sasaki, K.; Joslyn, C. M.; Kim, A. S.; Cavallaro, C. L.; Lawrence, R. M.; Johnson, S. R.; et al. Ligand and Target Discovery by Fragment-Based Screening in Human Cells. *Cell* **2017**, *168* (3), 527-541.e529. DOI: 10.1016/j.cell.2016.12.029 From NLM.
(27) Luo, M.; Spradlin, J. N.; Boike, L.; Tong, B.; Brittain, S. M.; McKenna, J. M.; Tallarico, J. A.; Schirle, M.; Maimone, T. J.; Nomura, D. K. Chemoproteomics-enabled discovery of covalent RNF114-based degraders that mimic natural product function. *Cell Chem Biol* **2021**, *28* (4), 559-566 e515. DOI: 10.1016/j.chembiol.2021.01.005.
(28) Zhang, X. Y.; Crowley, V. M.; Wucherpfennig, T. G.; Dix, M. M.; Cravatt, B. F. Electrophilic PROTACs that degrade nuclear proteins by engaging DCAF16. *Nat Chem Biol* **2019**, *15* (7), 737-+. DOI: 10.1038/s41589-019-0279-5.
(29) Lee, H.; Lee, J. Y.; Jang, H.; Cho, H. Y.; Kang, M.; Bae, S. H.; Kim, S.; Kim, E.; Jang, J.; Kim, J. Y.; et al. Discovery of proteolysis-targeting chimera targeting undruggable proteins using a covalent ligand screening approach. *Eur J Med Chem* **2024**, *263*, 115929. DOI: https://doi.org/10.1016/j.ejmech.2023.115929.
(30) Hanafi, M.; Chen, X.; Neamati, N. Discovery of a Napabucasin PROTAC as an Effective Degrader of the E3 Ligase ZFP91. *Journal of Medicinal Chemistry* **2021**, *64* (3), 1626-1648. DOI: 10.1021/acs.jmedchem.0c01897.
(31) Bondeson, D. P.; Smith, B. E.; Burslem, G. M.; Buhimschi, A. D.; Hines, J.; Jaime-Figueroa, S.; Wang, J.; Hamman, B. D.; Ishchenko, A.; Crews, C. M. Lessons in PROTAC Design from Selective Degradation with a Promiscuous Warhead. *Cell Chem Biol* **2018**, *25* (1), 78-87.e75. DOI: 10.1016/j.chembiol.2017.09.010 From NLM.
(32) Khan, S.; Zhang, X.; Lv, D.; Zhang, Q.; He, Y.; Zhang, P.; Liu, X.; Thummuri, D.; Yuan, Y.; Wiegand, J. S.; et al. A selective BCL-X(L) PROTAC degrader achieves safe and potent antitumor activity. *Nat Med* **2019**, *25* (12), 1938-1947. DOI: 10.1038/s41591-019-0668-z From NLM.
(33) Zalewska, M.; Trefon, J.; Milnerowicz, H. The role of metallothionein interactions with other proteins. *Proteomics* **2014**, *14* (11), 1343-1356. DOI: 10.1002/pmic.201300496.
(34) Jin, R.; Chow, V. T. K.; Tan, P.-H.; Dheen, S. T.; Duan, W.; Bay, B.-H. Metallothionein 2A expression is associated with cell proliferation in breast cancer. *Carcinogenesis* **2002**, *23* (1), 81-86. DOI: 10.1093/carcin/23.1.81 (acccessed 5/5/2022).
(35) Kim, H. G.; Kim, J. Y.; Han, E. H.; Hwang, Y. P.; Choi, J. H.; Park, B. H.; Jeong, H. G. Metallothionein-2A overexpression increases the expression of matrix metalloproteinase-9 and invasion of breast cancer cells. *FEBS Lett* **2011**, *585* (2), 421-428. DOI: 10.1016/j.febslet.2010.12.030.
(36) Lim, D.; Jocelyn, K. M.; Yip, G. W.; Bay, B. H. Silencing the Metallothionein-2A gene inhibits cell cycle progression from G1- to S-phase involving ATM and cdc25A signaling in breast cancer cells. *Cancer Lett* **2009**, *276* (1), 109-117. DOI: 10.1016/j.canlet.2008.10.038.
(37) Si, M.; Lang, J. The roles of metallothioneins in carcinogenesis. *J Hematol Oncol* **2018**, *11* (1), 107. DOI: 10.1186/s13045-018-0645-x.
(38) Peris-Díaz, M. D.; Guran, R.; Domene, C.; de los Rios, V.; Zitka, O.; Adam, V.; Krężel, A. An Integrated Mass Spectrometry and Molecular Dynamics Simulations Approach Reveals the Spatial Organization Impact of Metal-Binding Sites on the Stability of Metal-Depleted Metallothionein-2 Species. *Journal of the American Chemical Society* **2021**, *143* (40), 16486-16501. DOI: 10.1021/jacs.1c05495.
(39) Korkola, N. C.; Stillman, M. J. Structural Role of Cadmium and Zinc in Metallothionein Oxidation by Hydrogen Peroxide: The Resilience of Metal–Thiolate Clusters. *Journal of the American Chemical Society* **2023**, *145* (11), 6383-6397. DOI: 10.1021/jacs.2c13578.
(40) Mangelinck, A.; da Costa, M. E. M.; Stefanovska, B.; Bawa, O.; Polrot, M.; Gaspar, N.; Fromigué, O. MT2A is an early predictive biomarker of response to chemotherapy and a potential therapeutic target in osteosarcoma. *Scientific Reports* **2019**, *9* (1), 12301. DOI: 10.1038/s41598-019-48846-2.
(41) Lim, D.; Jocelyn, K. M.-X.; Yip, G. W.-C.; Bay, B.-H. Silencing the Metallothionein-2A gene inhibits cell cycle progression from G1- to S-phase involving ATM and cdc25A signaling in breast cancer cells. *Cancer Letters* **2009**, *276* (1), 109-117. DOI: https://doi.org/10.1016/j.canlet.2008.10.038.
(42) Masiulionytė, B.; Valiulytė, I.; Tamašauskas, A.; Skiriutė, D. Metallothionein Genes are Highly Expressed in Malignant Astrocytomas and Associated with Patient Survival. *Scientific Reports* **2019**, *9* (1), 5406. DOI: 10.1038/s41598-019-41974-9.
(43) Borchert, S.; Suckrau, P.-M.; Walter, R. F. H.; Wessolly, M.; Mairinger, E.; Steinborn, J.; Hegedus, B.; Hager, T.; Herold, T.; Eberhardt, W. E. E.; et al. Impact of metallothionein-knockdown on cisplatin resistance in malignant pleural mesothelioma. *Scientific Reports* **2020**, *10* (1), 18677. DOI: 10.1038/s41598-020-75807-x.
(44) Borchert, S.; Suckrau, P.-M.; Walter, R. F. H.; Wessolly, M.; Mairinger, E.; Steinborn, J.; Hegedus, B.; Hager, T.; Herold, T.; Eberhardt, W. E. E.; et al. Impact of metallothionein-knockdown on cisplatin resistance in malignant pleural mesothelioma. In *Scientific reports*, 2020; Vol. 10, p 18677.
(45) Tekur, S.; Ho, S.-M. Ribozyme-mediated downregulation of human metallothionein IIa induces apoptosis in human prostate and ovarian cancer cell lines. *Molecular Carcinogenesis* **2002**, *33* (1), 44-55. DOI: https://doi.org/10.1002/mc.10017 (acccessed 2024/03/01).
(46) Cui, C.; Dwyer, B. G.; Liu, C.; Abegg, D.; Cai, Z.-J.; Hoch, D. G.; Yin, X.; Qiu, N.; Liu, J.-Q.; Adibekian, A.; et al. Total Synthesis and Target Identification of the Curcusone Diterpenes. *Journal of the American Chemical Society* **2021**, *143* (11), 4379-4386. DOI: 10.1021/jacs.1c00557.
(47) Hoch, D. G.; Abegg, D.; Hannich, J. T.; Pechalrieu, D.; Shuster, A.; Dwyer, B. G.; Wang, C.; Zhang, X.; You, Q.; Riezman, H.; et al. Combined Omics Approach Identifies Gambogic Acid and Related Xanthones as Covalent Inhibitors of the Serine

Palmitoyltransferase Complex. *Cell Chemical Biology* **2020**, *27* (5), 586-597.e512. DOI: https://doi.org/10.1016/j.chembiol.2020.03.008.
(48) Wang, C.; Abegg, D.; Hoch, D. G.; Adibekian, A. Chemoproteomics-Enabled Discovery of a Potent and Selective Inhibitor of the DNA Repair Protein MGMT. *Angewandte Chemie International Edition* **2016**, *55* (8), 2911-2915. DOI: https://doi.org/10.1002/anie.201511301 (acccessed 2024/06/17).
(49) Zambaldo, C.; Vinogradova, E. V.; Qi, X.; Iaconelli, J.; Suciu, R. M.; Koh, M.; Senkane, K.; Chadwick, S. R.; Sanchez, B. B.; Chen, J. S.; et al. 2-Sulfonylpyridines as Tunable, Cysteine-Reactive Electrophiles. *Journal of the American Chemical Society* **2020**, *142* (19), 8972-8979. DOI: 10.1021/jacs.0c02721.
(50) Castellón, J. O.; Ofori, S.; Burton, N. R.; Julio, A. R.; Turmon, A. C.; Armenta, E.; Sandoval, C.; Boatner, L. M.; Takayoshi, E. E.; Faragalla, M.; et al. Chemoproteomics Identifies State-Dependent and Proteoform-Selective Caspase-2 Inhibitors. *Journal of the American Chemical Society* **2024**, *146* (22), 14972-14988. DOI: 10.1021/jacs.3c12240.
(51) Bond, M. J.; Chu, L.; Nalawansha, D. A.; Li, K.; Crews, C. M. Targeted Degradation of Oncogenic KRAS(G12C) by VHL-Recruiting PROTACs. *Acs Central Sci* **2020**, *6* (8), 1367-1375. DOI: 10.1021/acscentsci.0c00411.
(52) Qiu, N.; Pechalrieu, D.; Abegg, D.; Adibekian, A. Chemoproteomic Profiling Maps Zinc-Dependent Cysteine Reactivity. *Chemical Research in Toxicology* **2024**, *37* (4), 620-632. DOI: 10.1021/acs.chemrestox.3c00416.
(53) Fan, L. Z.; Cherian, M. G. Potential role of p53 on metallothionein induction in human epithelial breast cancer cells. *Br J Cancer* **2002**, *87* (9), 1019-1026. DOI: 10.1038/sj.bjc.6600549.
(54) Shimoda, R.; Achanzar, W. E.; Qu, W.; Nagamine, T.; Takagi, H.; Mori, M.; Waalkes, M. P. Metallothionein is a potential negative regulator of apoptosis. *Toxicol Sci* **2003**, *73* (2), 294-300. DOI: 10.1093/toxsci/kfg095.
(55) Borchert, S.; Suckrau, P. M.; Walter, R. F. H.; Wessolly, M.; Mairinger, E.; Steinborn, J.; Hegedus, B.; Hager, T.; Herold, T.; Eberhardt, W. E. E.; et al. Impact of metallothionein-knockdown on cisplatin resistance in malignant pleural mesothelioma. *Sci Rep* **2020**, *10* (1), 18677. DOI: 10.1038/s41598-020-75807-x.
(56) Dias, A. M.; de Mendonca, R. P.; Kataoka, M. S. D.; Jaeger, R. G.; Pinheiro, J. D. V.; Alves, S. D. Downregulation of metallothionein 2A reduces migration, invasion and proliferation activities in human squamous cell carcinoma cells. *Mol Biol Rep* **2022**. DOI: 10.1007/s11033-022-07206-6.
(57) Habel, N.; Hamidouche, Z.; Girault, I.; Patino-Garcia, A.; Lecanda, F.; Marie, P. J.; Fromigue, O. Zinc chelation: a metallothionein 2A's mechanism of action involved in osteosarcoma cell death and chemotherapy resistance. *Cell Death Dis* **2013**, *4*, e874. DOI: 10.1038/cddis.2013.405.
(58) Puca, R.; Nardinocchi, L.; Bossi, G.; Sacchi, A.; Rechavi, G.; Givol, D.; D'Orazi, G. Restoring wtp53 activity in HIPK2 depleted MCF7 cells by modulating metallothionein and zinc. *Exp Cell Res* **2009**, *315* (1), 67-75. DOI: 10.1016/j.yexcr.2008.10.018.
(59) Cyrus, K.; Wehenkel, M.; Choi, E. Y.; Han, H. J.; Lee, H.; Swanson, H.; Kim, K. B. Impact of linker length on the activity of PROTACs. *Mol Biosyst* **2011**, *7* (2), 359-364. DOI: 10.1039/c0mb00074d.
(60) Troup, R. I.; Fallan, C.; Baud, M. G. J. Current strategies for the design of PROTAC linkers: a critical review. *Exploration of Targeted Anti-tumor Therapy* **2020**, *1* (5), 273-312. DOI: 10.37349/etat.2020.00018.
(61) Tinworth, C. P.; Lithgow, H.; Dittus, L.; Bassi, Z. I.; Hughes, S. E.; Muelbaier, M.; Dai, H.; Smith, I. E. D.; Kerr, W. J.; Burley, G. A.; et al. PROTAC-Mediated Degradation of Bruton's Tyrosine Kinase Is Inhibited by Covalent Binding. *ACS Chem Biol* **2019**, *14* (3), 342-347. DOI: 10.1021/acschembio.8b01094.
(62) Bondeson, D. P.; Mares, A.; Smith, I. E.; Ko, E.; Campos, S.; Miah, A. H.; Mulholland, K. E.; Routly, N.; Buckley, D. L.; Gustafson, J. L.; et al. Catalytic in vivo protein knockdown by small-molecule PROTACs. *Nat Chem Biol* **2015**, *11* (8), 611-617. DOI: 10.1038/nchembio.1858.
(63) Cromm, P. M.; Samarasinghe, K. T. G.; Hines, J.; Crews, C. M. Addressing Kinase-Independent Functions of Fak via PROTAC-Mediated Degradation. *Journal of the American Chemical Society* **2018**, *140* (49), 17019-17026. DOI: 10.1021/jacs.8b08008.
(64) Niu, T.; Li, K. L.; Jiang, L.; Zhou, Z. S.; Hong, J.; Chen, X. K.; Dong, X. W.; He, Q. J.; Cao, J.; Yang, B.; et al. Noncovalent CDK12/13 dual inhibitors-based PROTACs degrade CDK12-Cyclin K complex and induce synthetic lethality with PARP inhibitor. *Eur J Med Chem* **2022**, *228*. DOI: ARTN 114012

10.1016/j.ejmech.2021.114012.
(65) Ryu, H. H.; Jung, S.; Jung, T. Y.; Moon, K. S.; Kim, I. Y.; Jeong, Y. I.; Jin, S. G.; Pei, J.; Wen, M.; Jang, W. Y. Role of metallothionein 1E in the migration and invasion of human glioma cell lines. *Int J Oncol* **2012**, *41* (4), 1305-1313. DOI: 10.3892/ijo.2012.1570.
(66) Anson, K. J.; Corbet, G. A.; Palmer, A. E. Zn(2+) influx activates ERK and Akt signaling pathways. *Proc Natl Acad Sci U S A* **2021**, *118* (11). DOI: 10.1073/pnas.2015786118.
(67) Arriaga, J. M.; Greco, A.; Mordoh, J.; Bianchini, M. Metallothionein 1G and zinc sensitize human colorectal cancer cells to chemotherapy. *Mol Cancer Ther* **2014**, *13* (5), 1369-1381. DOI: 10.1158/1535-7163.MCT-13-0944.
(68) Meplan, C.; Richard, M. J.; Hainaut, P. Metalloregulation of the tumor suppressor protein p53: zinc mediates the renaturation of p53 after exposure to metal chelators in vitro and in intact cells. *Oncogene* **2000**, *19* (46), 5227-5236. DOI: 10.1038/sj.onc.1203907.
(69) Zeng, J.; Vallee, B. L.; Kägi, J. H. Zinc transfer from transcription factor IIIA fingers to thionein clusters. *P Natl Acad Sci USA* **1991**, *88* (22), 9984-9988. DOI: 10.1073/pnas.88.22.9984 PubMed.
(70) Dong, L.; Li, Z. J.; Xue, L. Y.; Li, G.; Zhang, C. Y.; Cai, Z. H.; Li, H.; Guo, R. F. DIAPH3 promoted the growth, migration and metastasis of hepatocellular carcinoma cells by activating beta-catenin/TCF signaling. *Mol Cell Biochem* **2018**, *438* (1-2), 183-190. DOI: 10.1007/s11010-017-3125-7.
(71) Rong, Y. F.; Gao, J.; Kuang, T. T.; Chen, J. L.; Li, J. A.; Huang, Y. F.; Xin, H. G.; Fang, Y.; Han, X.; Sun, L. Q.; et al. DIAPH3 promotes pancreatic cancer progression by activating selenoprotein TrxR1-mediated antioxidant effects. *J Cell Mol Med* **2021**, *25* (4), 2163-2175. DOI: 10.1111/jcmm.16196.
(72) Jurmeister, S.; Baumann, M.; Balwierz, A.; Keklikoglou, I.; Ward, A.; Uhlmann, S.; Zhang, J. D.; Wiemann, S.; Sahin, Ö. MicroRNA-200c represses migration and invasion of breast cancer cells by targeting actin-regulatory proteins FHOD1 and PPM1F. *Mol Cell Biol* **2012**, *32* (3), 633-651. DOI: 10.1128/MCB.06212-11 PubMed.

(73) Gan, Z.; Ding, L.; Burckhardt, C. J.; Lowery, J.; Zaritsky, A.; Sitterley, K.; Mota, A.; Costigliola, N.; Starker, C. G.; Voytas, D. F.; et al. Vimentin Intermediate Filaments Template Microtubule Networks to Enhance Persistence in Cell Polarity and Directed Migration. *Cell Syst* **2016**, *3* (3), 252-263.e258. DOI: 10.1016/j.cels.2016.08.007 PubMed.
(74) Xuan, B. T.; Ghosh, D.; Jiang, J.; Shao, R.; Dawson, M. R. Vimentin filaments drive migratory persistence in polyploidal cancer cells. *P Natl Acad Sci USA* **2020**, *117* (43), 26756-26765. DOI: 10.1073/pnas.2011912117.
(75) Brulet, J. W.; Borne, A. L.; Yuan, K.; Libby, A. H.; Hsu, K.-L. Liganding Functional Tyrosine Sites on Proteins Using Sulfur–Triazole Exchange Chemistry. *Journal of the American Chemical Society* **2020**, *142* (18), 8270-8280. DOI: 10.1021/jacs.0c00648.
(76) Tarapore, P.; Shu, Y.; Guo, P.; Ho, S. M. Application of phi29 motor pRNA for targeted therapeutic delivery of siRNA silencing metallothionein-IIA and survivin in ovarian cancers. *Mol Ther* **2011**, *19* (2), 386-394. DOI: 10.1038/mt.2010.243.
(77) Lee, J. H.; Chae, J. W.; Kim, J. K.; Kim, H. J.; Chung, J. Y.; Kim, Y. H. Inhibition of cisplatin-resistance by RNA interference targeting metallothionein using reducible oligo-peptoplex. *J Control Release* **2015**, *215*, 82-90. DOI: 10.1016/j.jconrel.2015.07.015.
(78) Tekur, S.; Ho, S. M. Ribozyme-mediated downregulation of human metallothionein II(a) induces apoptosis in human prostate and ovarian cancer cell lines. *Mol Carcinog* **2002**, *33* (1), 44-55. DOI: 10.1002/mc.10017.
(79) Cardoso, S. V.; Silveira-Junior, J. B.; De Carvalho Machado, V.; De-Paula, A. M.; Loyola, A. M.; De Aguiar, M. C. Expression of metallothionein and p53 antigens are correlated in oral squamous cell carcinoma. *Anticancer Res* **2009**, *29* (4), 1189-1193.
(80) Liu, Z.; Ye, Q.; Wu, L.; Gao, F.; Xie, H.; Zhou, L.; Zheng, S.; Xu, X. Metallothionein 1 family profiling identifies MT1X as a tumor suppressor involved in the progression and metastastatic capacity of hepatocellular carcinoma. *Mol Carcinog* **2018**, *57* (11), 1435-1444. DOI: 10.1002/mc.22846.
(81) Yamasaki, M.; Nomura, T.; Sato, F.; Mimata, H. Metallothionein is up-regulated under hypoxia and promotes the survival of human prostate cancer cells. *Oncol Rep* **2007**, *18* (5), 1145-1153.
(82) Abdel-Mageed, A. B.; Agrawal, K. C. Activation of nuclear factor kappa B: Potential role in metallothionein-mediated mitogenic response. *Cancer Res* **1998**, *58* (11), 2335-2338.
(83) Park, L.; Min, D.; Kim, H.; Park, J.; Choi, S.; Park, Y. The combination of metallothionein and superoxide dismutase protects pancreatic beta cells from oxidative damage. *Diabetes-Metab Res* **2011**, *27* (8), 802-808. DOI: 10.1002/dmrr.1254.
(84) West, A. K.; Leung, J. Y. K.; Chung, R. S. Neuroprotection and regeneration by extracellular metallothionein via lipoprotein-receptor-related proteins. *J Biol Inorg Chem* **2011**, *16* (7), 1115-1122. DOI: 10.1007/s00775-011-0817-4.